8.3. Summer Circulation and Upwelling

During summer (January to March), strong south-easterly winds over the shelf offshore from the mouth of the gulf create an upwelling favourable environment that results in cooler surface water residing off Eyre Peninsula and south-west Kangaroo Island (Middleton and Bye 2007). This upwelled water is hypothesized to have its origin in slope waters south of Kangaroo Island and may be a potential source of nutrients if advected into Spencer Gulf and the TFZ area. Strong upwelling favourable winds were observed during January and early February 2006 (Figure 6.3.2), with associated upwelling evident.

The model shows cooler bottom water residing at the open boundary, with a cooler pool adjacent to the west of Yorke Peninsula (Figure 8.3.1). Cool water is not observed to strongly intrude into the TFZ region (the local model domain), although a temperature drop is observed around January 28th in bottom waters off Cape Donnington (Figure 8.3.2). Diurnal variability is observed to be evident during this period, associated with diurnal heating and convective cooling due to the surface heat flux. This temperature drop was also observed in modelled and measured data at mooring site M5 (Figure 8.3.3). The February 11th CTD transect (Figure 6.3.5-6.3.6) also indicates the existence of an onshore subsurface plume of cold fresh water. No clear propagation of a cool plume was observed into the TFZ region, indicating advection of upwelled water probably did not play a dominant role in decreasing bottom temperature during this time. However, we note that the calculated synthetic temperature presented in Section 6.3 is too warm, indicating that atmospheric heating alone is insufficient to account for the lower observed temperatures. That is, advection of cool water into the region may also be important.

In order to assess the role of advection during the upwelling period, the regional model was simulated with a passive tracer initialized to zero and having an open boundary condition equivalent to that of temperature. Two experiments are considered. In the first, the model is initialized on September 1st 2005 and results are presented for January 1st 2006. During this period, the winds are strongly from the north-west (Figure 6.3.2) and for the shelf are downwelling favourable. For the gulf mouth, such winds will drive a cyclonic (clockwise) circulation at the lower part of the gulf and near the mouth (Section 6.4; Middleton and Teixeira 2008). The result of this circulation on the passive tracer is evident in Figure 8.3.4. Results show that there is a gradual inflow of water on the western side of the gulf from October onwards (Figure 8.3.4).

Now consider the results of a second experiment with the passive tracer initialised using the open boundary temperature on January 1st 2006. The results are presented for JD 5935 (end of March) when the upwelling favourable winds cease (Figure 6.3.2). The results at this time show (Figure 8.3.5) an anticlockwise circulation near the gulf mouth with upwelled water moving from the shelf, east gulf coast and past the TFZ region.

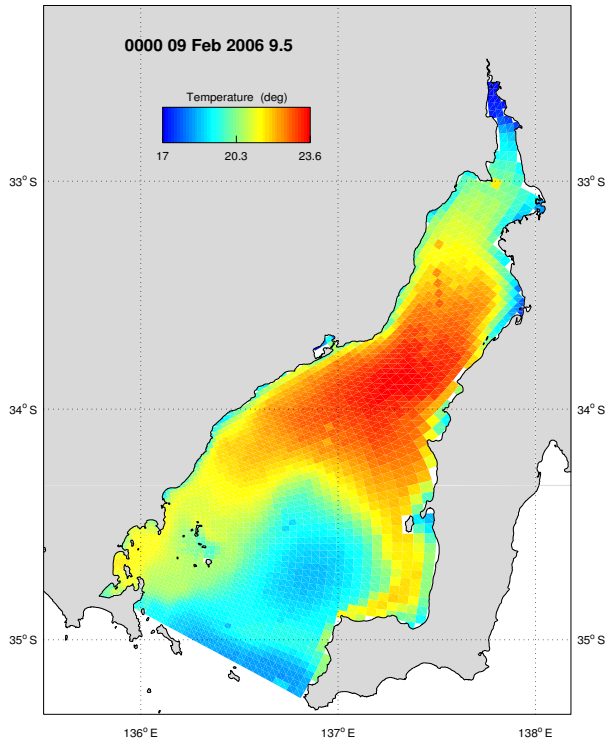

Figure 8.3.1. Regional modelled bottom temperature.

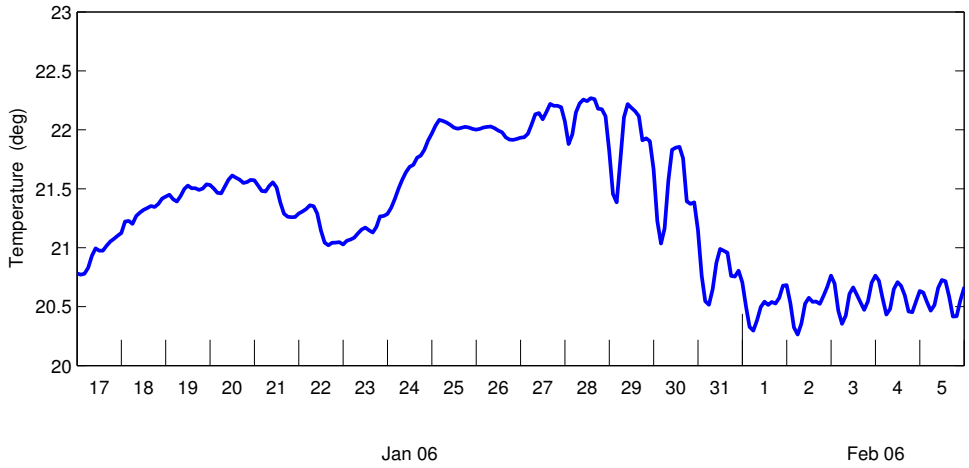

Figure 8.3.2. Modelled time series of bottom temperature off Cape Donnington.

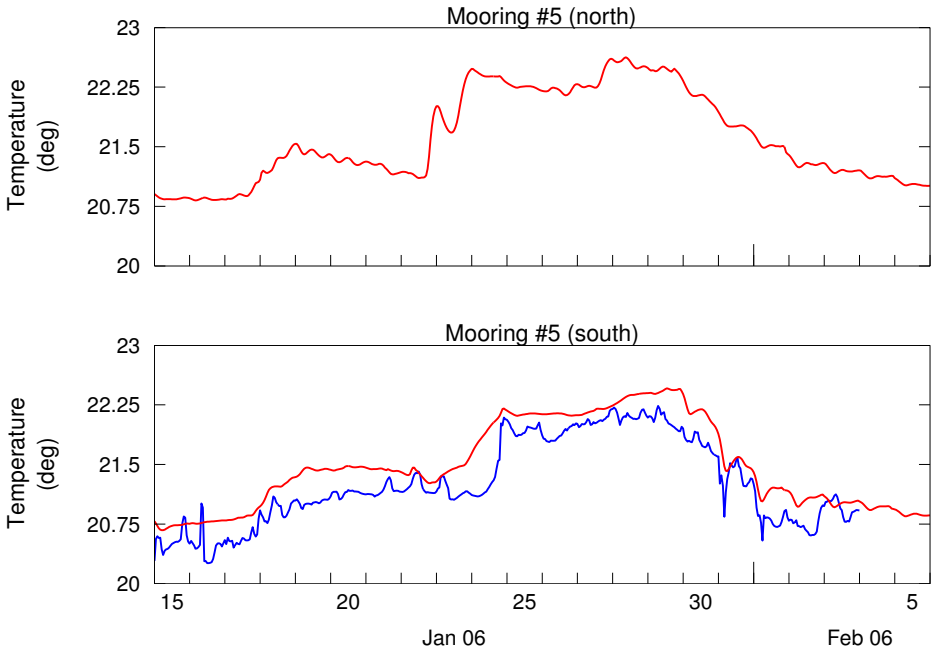

Figure 8.3.3. Measured (blue) and modelled (red) time series of temperature at Mooring #5.

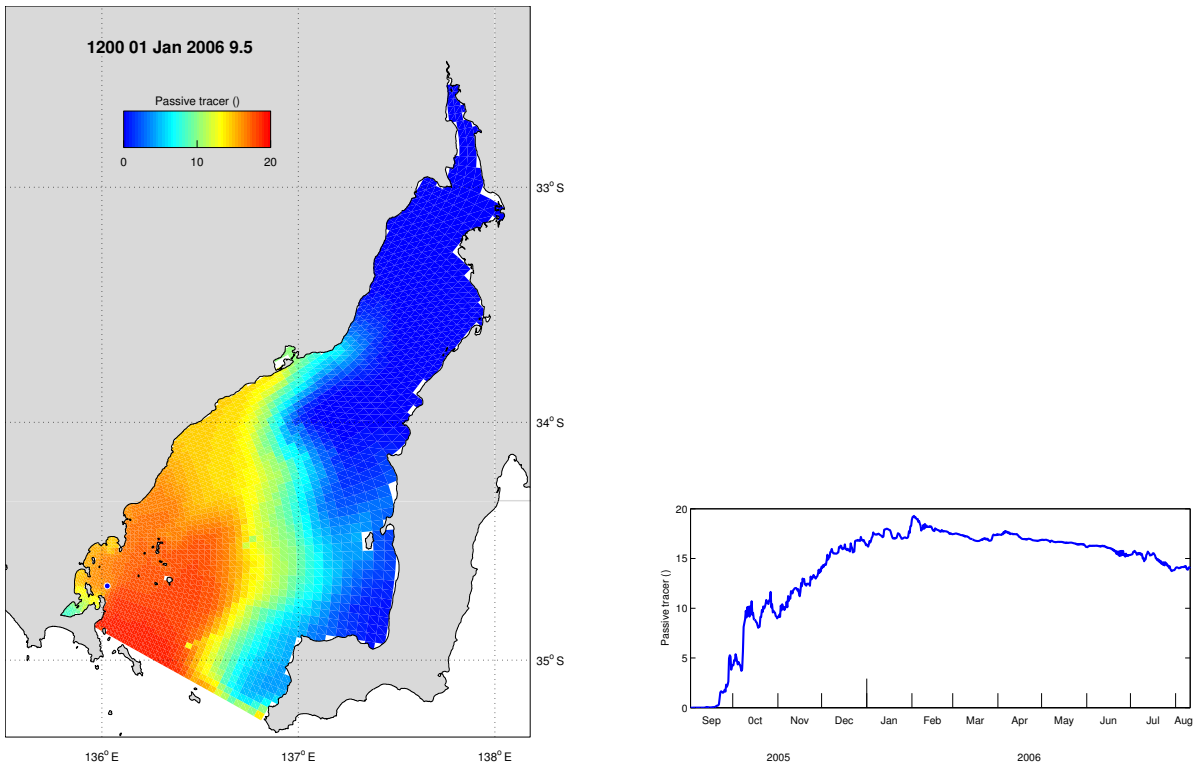

(a) Bottom temperature (b) Bottom time series in at Cape Donnington.

Figure 8.3.4. Passive tracer distribution using temperature open boundary condition to illustrate advective effects.

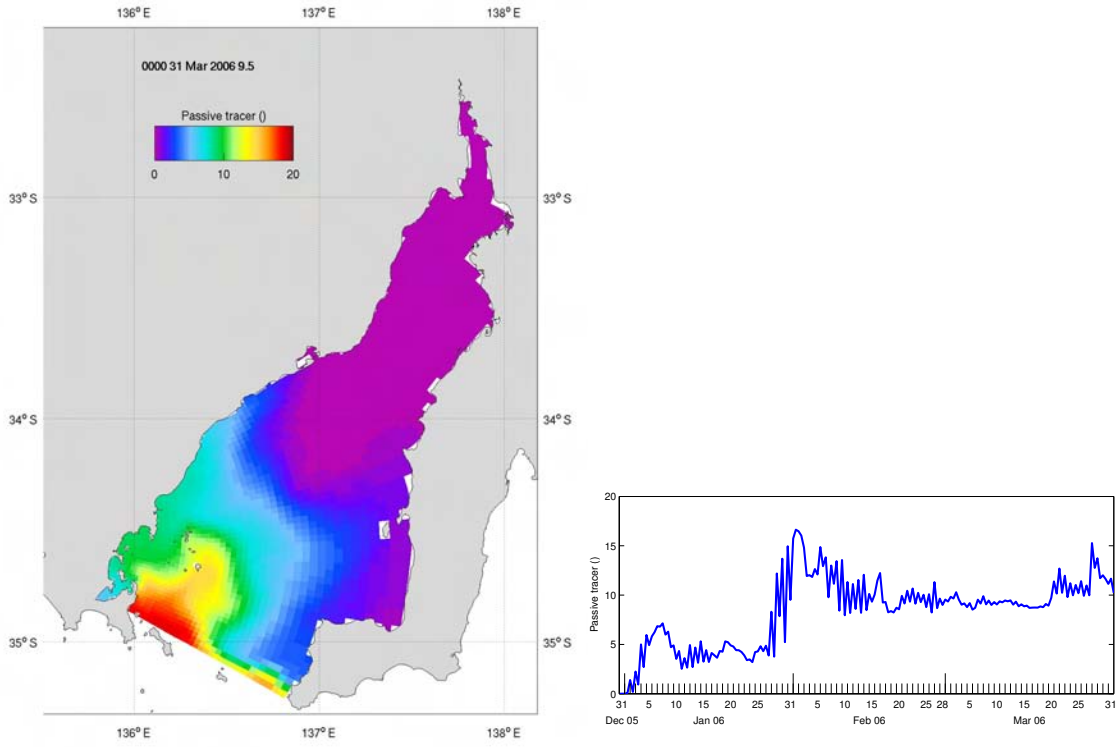

(a) Bottom temperature (b) Bottom time series in at Cape Donnington.

Figure 8.3.5. Passive tracer distribution initialised in January 2005, using temperature open boundary conditions to illustrate advective effects.

8.4. Flushing Characteristics

Passive tracers were used to obtain an estimate of the flushing characteristics of various regions around the TFZ. A passive tracer was initialised in a sub-region with a concentration of 1 and zero elsewhere, and the total mass in this sub-region was calculated throughout the simulation. Full forcing was applied to the domain (i.e. wind, tide, low frequency sea level and temperature / salinity effects). The e-folding time for flushing this sub-region is encountered when the total mass was reduced to 1/e (~38%) of the initial mass. This representation of the flushing time assumes that tracer is well mixed in the sub-region and the total mass is assumed to decrease exponentially according to:

$$M(t) = M_0 e^{-t/\tau} \qquad 8.4.1$$

where M_0 is the initial mass and τ is the flushing time scale (Tartinville et al, 1997). When $M = M_0/e$ then $t = \tau$, hence the flushing time can be recovered.

Summer (January 2006) flushing times for various sub-regions of the domain are displayed in Figures 8.4.1 to 8.4.6. These figures include the initial tracer distribution which defines the sub-region, the tracer distribution at the flushing time, and the temporal evolution of normalized total mass in the sub-region. The flushing times are tabulated in Table 8.4.1; included in this table are the flushing times for the various sub-regions during winter (July 2006). The general trend of tracer decrease is obtained by fitting a 2nd or 3rd order polynomial to the total mass, which aids in identifying the time τ when total mass is reduced to 1/e. The exponential curve of equation 8.4.1 is also fitted to the data, using the time scale τ identified from the polynomial fit.

Table 8.4.1 indicates that there exists a wide range of flushing times depending on which region is flushed. The computed flushing estimates are a somewhat subjective measure of exchange, since there are various methods of computing flushing (e.g. Tartinville et al, 1997) which may potentially yield different results, and the assumptions made in deriving flushing times are often violated. The final tracer concentration distributions clearly show that tracer is not always well mixed throughout the flushing region, hence flushing estimates may be compromised. The forcing in effect also has a large impact on the flushing rate; computations for a different time period under the influence of differing wind, heatflux and tidal conditions are expected to produce different flushing times. During the computation of these flushing times winds were relatively strong (5 – 10 m s^{-1}) southerly to south-easterly during the end of the neap tide (minimum neap tide on 8th January) with maximum spring tides around 16th January. Therefore the flushing times presented in Table 8.4.1 should be treated with caution, and should not be assumed to be a definitive measure. They are, however, a useful indication of the relative flushing rates of various regions within the domain.

Proper Bay appears to have poor connectivity with the remainder of the domain and consequently has relatively slow flushing. Boston Island diminishes the connectivity of the bay westwards of the island with open water to the east, resulting in longer flushing times than Louth and Peake Bays. The zone encompassing the tuna farming region is also flushed relatively quickly, however, the tracer in this region has not exited the domain completely but rather has been re-distributed to other areas within the domain. This highlights one of the limitations of the application of these flushing estimates; the region in question may be

flushed, but the material flushed quite often is relocated to another area within the system and hence not completely removed. If tracer is distributed throughout the whole region then this is not possible, and reduction in total mass is only possible via transport through the open boundary resulting in the longest flushing estimate of ~14 days. This estimate is again dependent on the forcing in effect; using particle tracking provides a more accurate estimate of ~20 days for flushing the entire region (Section 8.6).

The winds imposed during the flushing calculations drove an onshore surface flow that was compensated with an offshore bottom flow, representing a downwelling situation. This was particularly evident in Louth Bay (Figure 8.4.7 a) and is reflected in the tracer distribution in Louth Bay, where tracer is rapidly subducted to lower levels in the water column and rapidly disappears from the surface layer (Figure 8.4.7 b).

Table 8.4.1. Flushing times.

Region	Flushing time (days)
Whole domain	13.9
Boston Bay	8.2
Proper Bay	10.8
Louth Bay	1.5
Peake Bay	2.7
Tuna zone	2.0

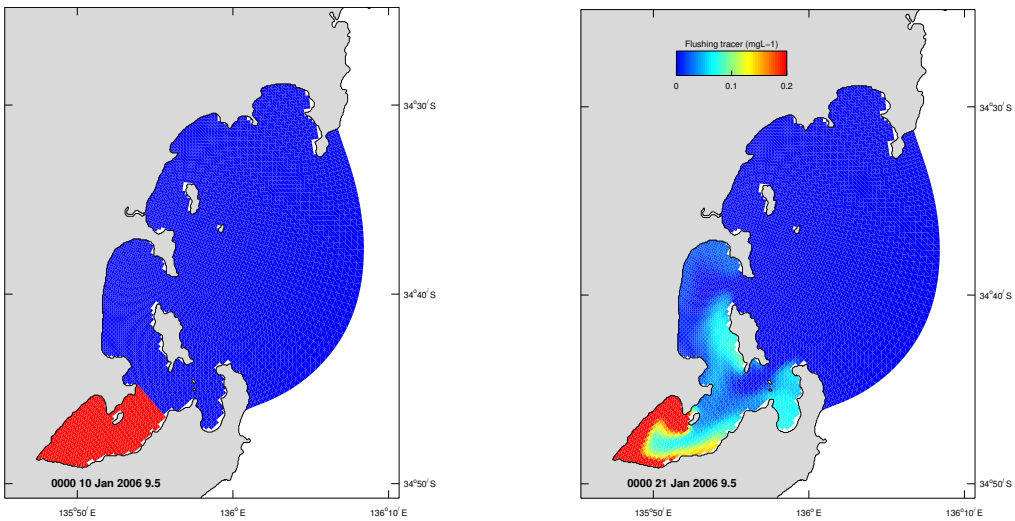

(a) Initial condition (b) Distribution at 11 days

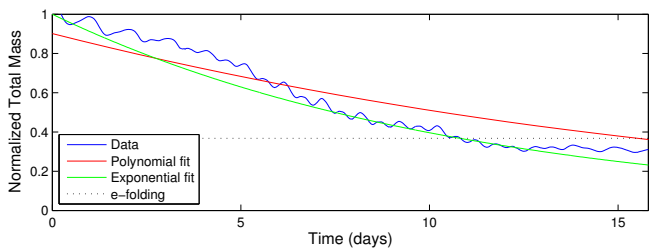

(c) Time series of total mass

Figure 8.4.1. Flushing for Proper Bay.

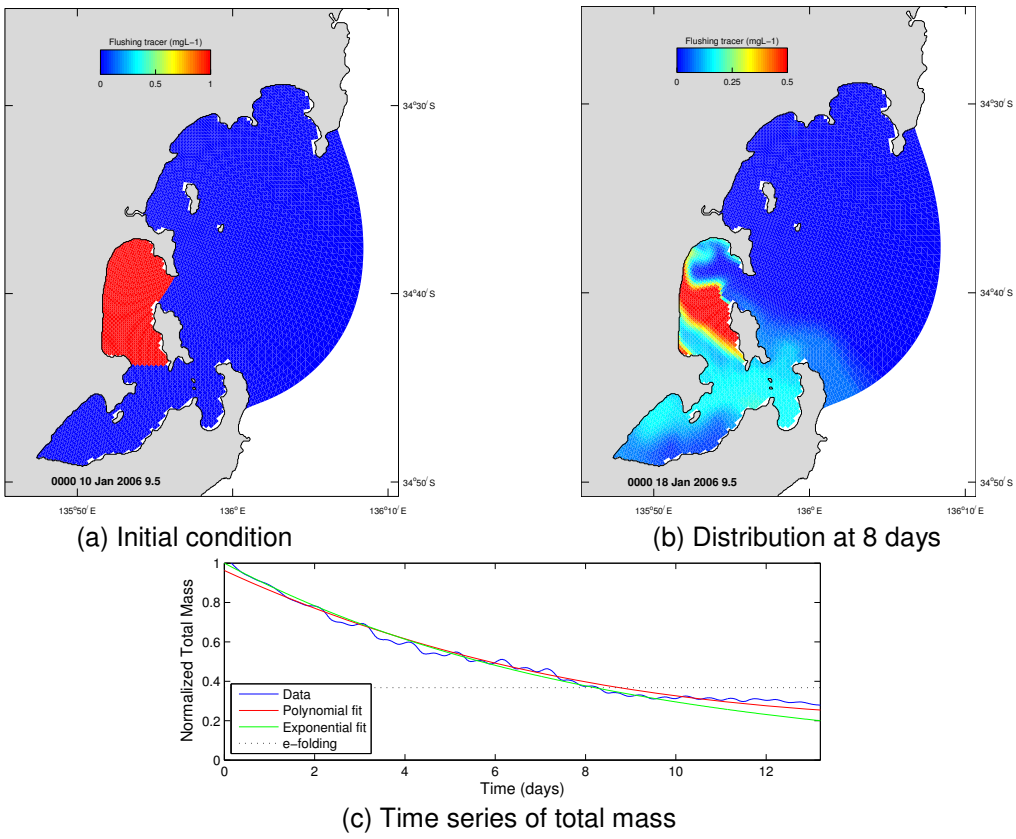

(a) Initial condition (b) Distribution at 8 days

(c) Time series of total mass

Figure 8.4.2. Flushing for Boston Bay.

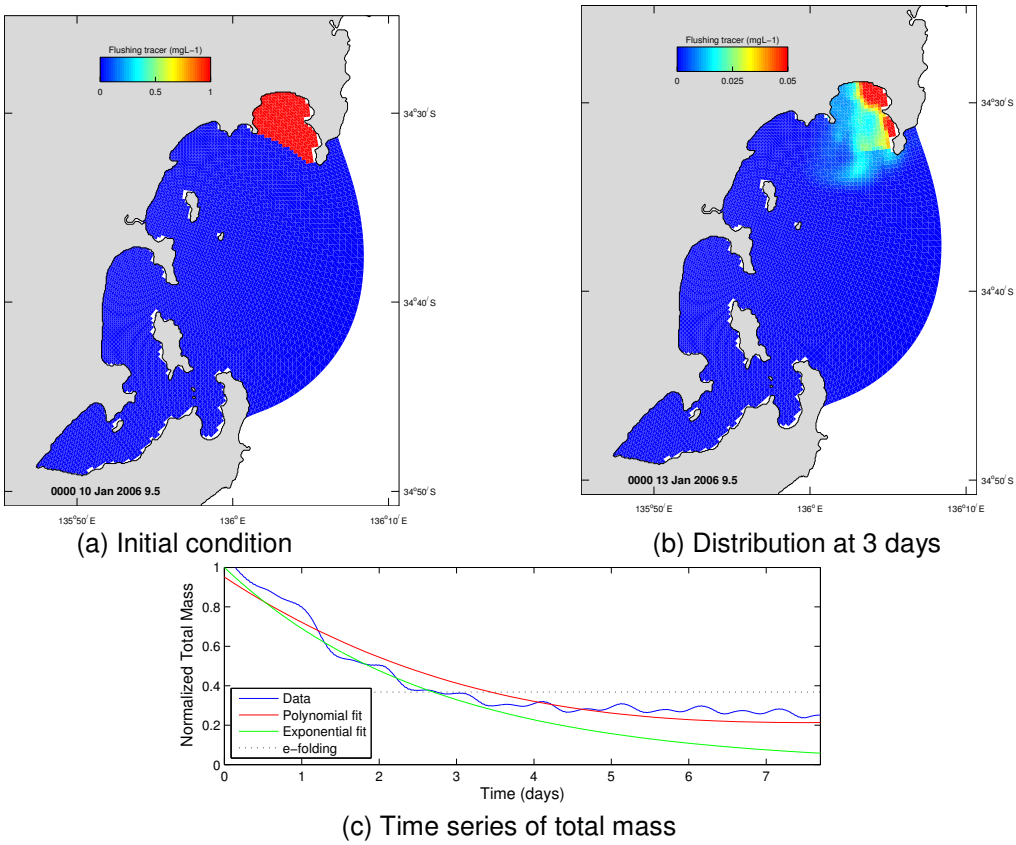

(a) Initial condition (b) Distribution at 3 days

(c) Time series of total mass

Figure 8.4.3. Flushing for Peake Bay.

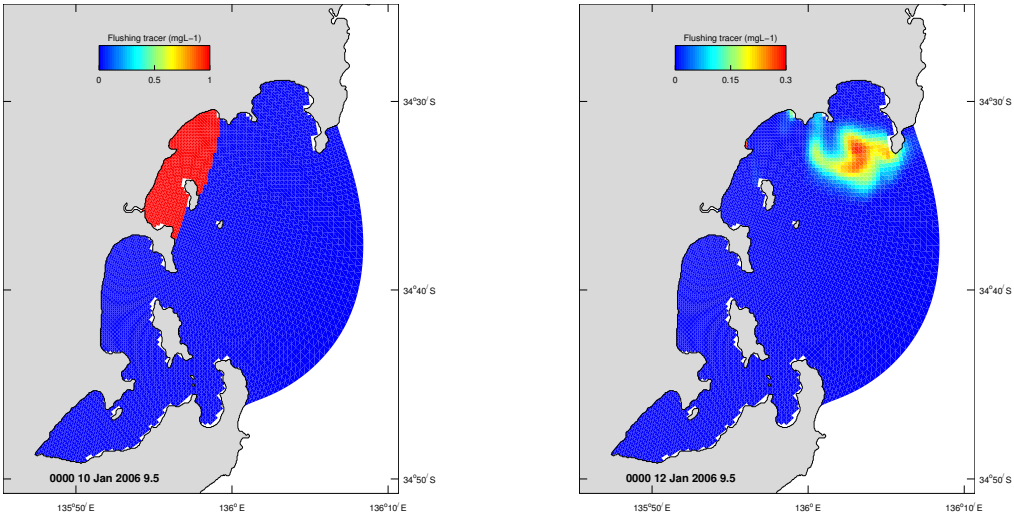

(a) Initial condition (b) Distribution at 2 days

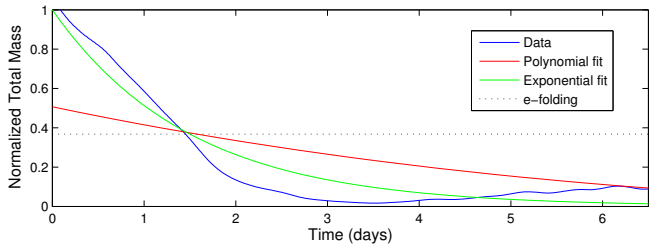

(c) Time series of total mass

Figure 8.4.4. Flushing for Louth Bay.

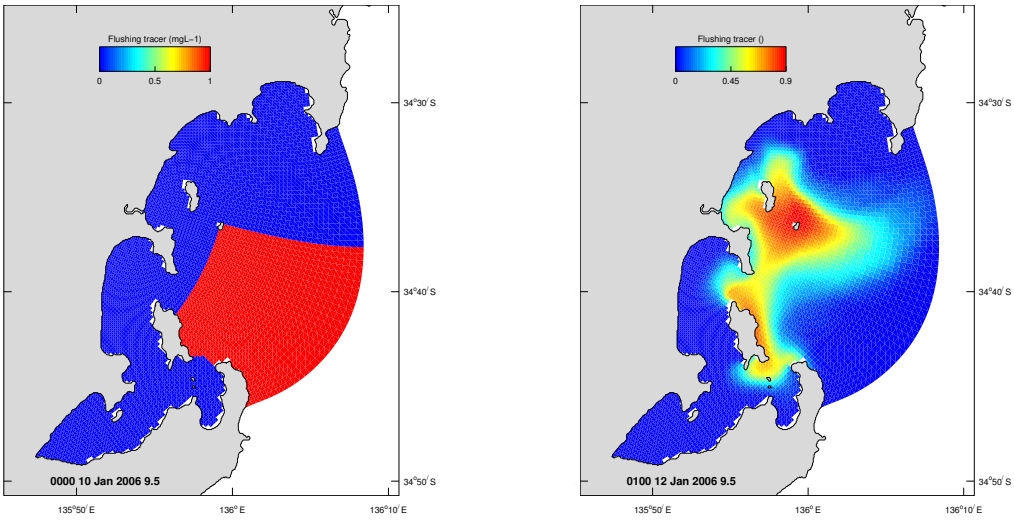

(a) Initial condition (b) Distribution at 2 days

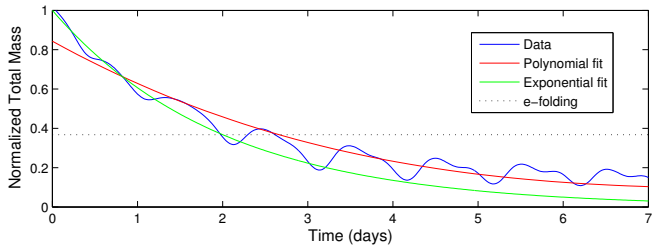

(c) Time series of total mass

Figure 8.4.5. Flushing for the TFZ region.

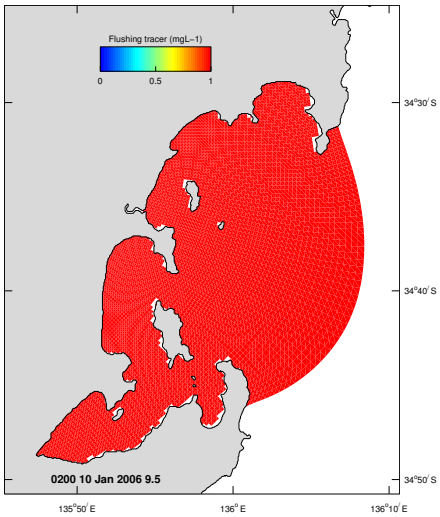

(a) Initial condition

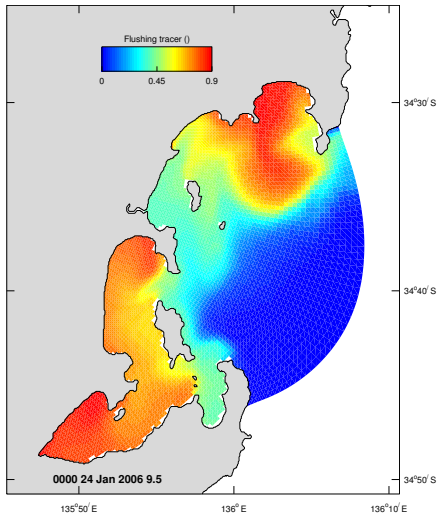

(b) Distribution at 14 days

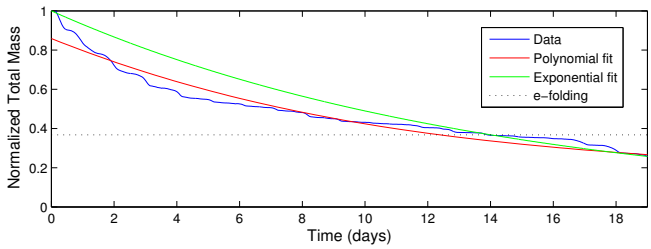

(c) Time series of total mass

Figure 8.4.6. Flushing for whole domain.

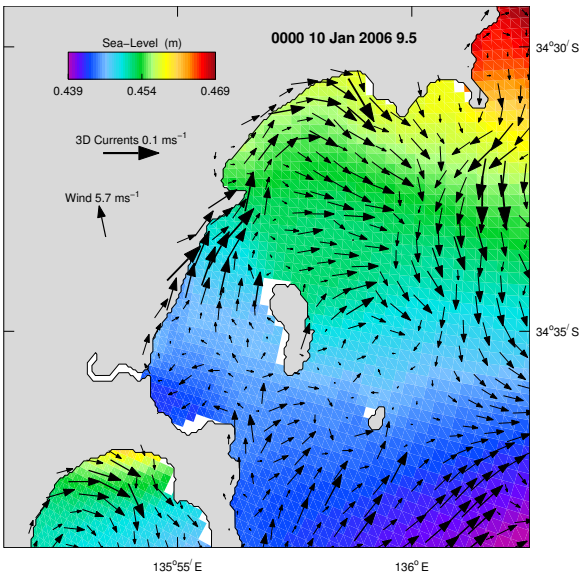

(a) Bottom flow

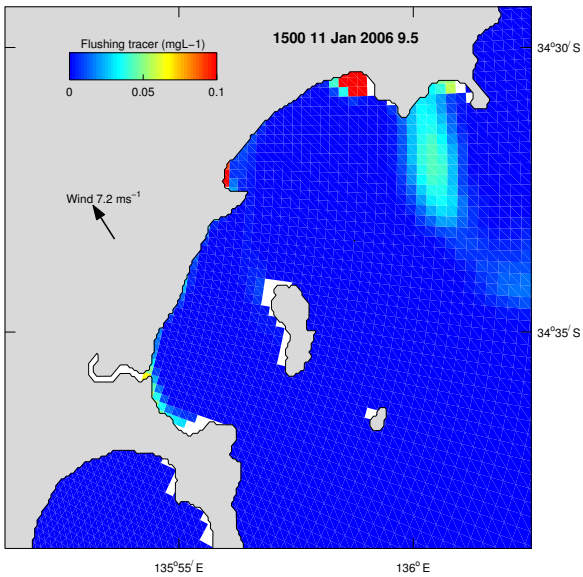

(b) Surface tracer distribution after 1.25 days

Figure 8.4.7. Flow characteristics demonstrating downwelling in Louth Bay.

8.5. Mixing zones

Point sources of tracers were continuously input into the water column at locations corresponding to a number of sites (Figure 8.5.1) with unit loads (assumed to be 1 g s^{-1} ~ 31,500 kg $year^{-1}$, giving output concentrations in units of gm^{-3}, or mgL^{-1}) for the 12 month simulation period of September 2005 - August 2006. Tracers were released into the top 1 m of the water column. The continuous tracer input will be advected and mixed to result in a quasi steady distribution, which will vary according to the forcing (wind, tide) in effect at any point in time. These distributions at any given time are not particularly useful to characterise the general tracer distribution, hence a statistical tracer distribution representing the whole simulation period was generated. Surface tracer distributions were output at 4 hour intervals and post-processed to compute the 5th, 50th (median) and 95th percentile concentration distributions for the whole simulation, providing a statistical description of the distributions resulting from tracer transport over this period. Owing to the volume of information that must be stored to compute the statistical distributions, only distributions for the surface layer were attempted and it was not feasible to create plots for bottom waters or along sections. Note that the response of the tracers to the interaction of the point source input with the system dynamics is linear, so that if the load were scaled by some arbitrary factor then the corresponding concentrations can be scaled accordingly.

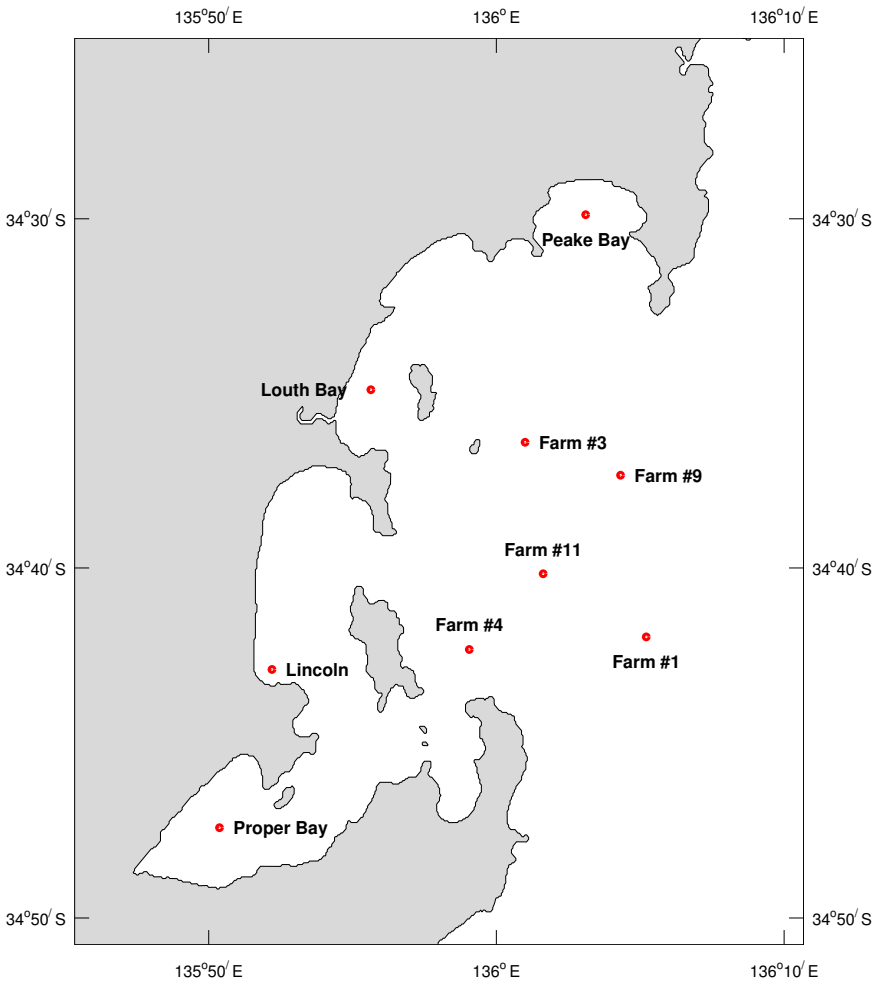

Figure 8.5.1. Point source release locations.

Results are displayed as Figures 8.5.2 to 8.5.11. Results are interpreted thus: given that a continuous unit load is input at the Port Lincoln site and its distribution throughout the domain allowed to reach quasi-steady state, at any given location in the domain one would expect to find the concentrations less than those shown in Figure 8.5.2 (a) for 5% of the time, less than those in Figure 8.5.2 (b) for 50% of the time and less than those in Figure 8.5.2 (c) for 95% of the time. These percentile plots provide a statistical description of the tracer concentration throughout the domain expected from various point source releases. Note that the concentration scales in the figures for the three percentiles generally differ from one another.

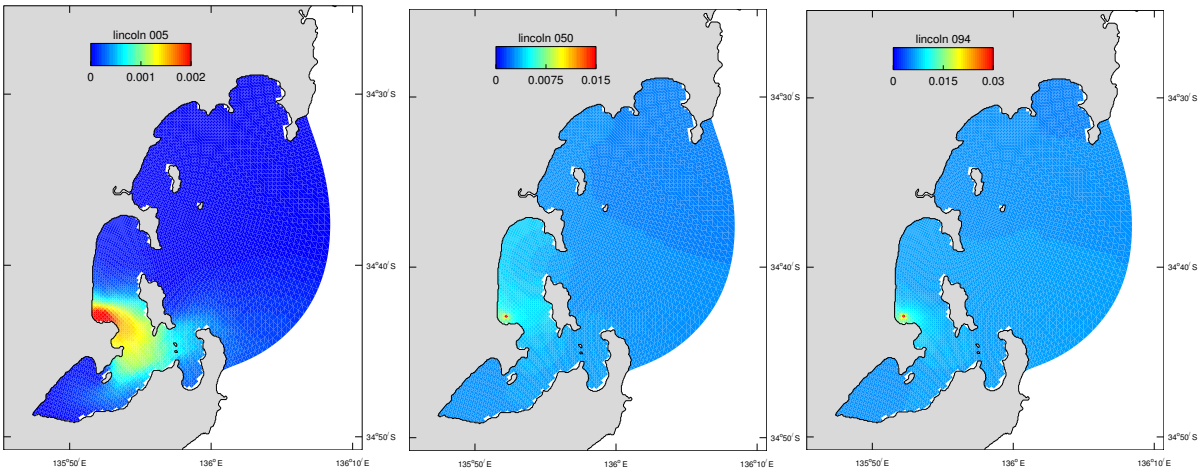

(a) 5 percentile (b) Median (c) 95 percentile

Figure 8.5.2. Quasi-steady state tracer distribution for Port Lincoln release.

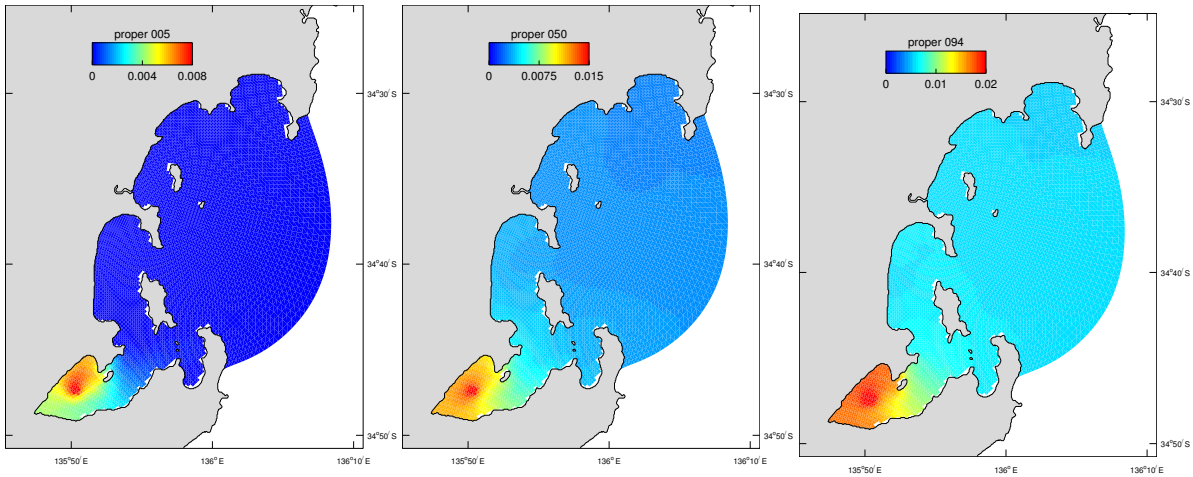

(a) 5 percentile (b) Median (c) 95 percentile

Figure 8.5.3. Quasi-steady state tracer distribution for Proper Bay release.

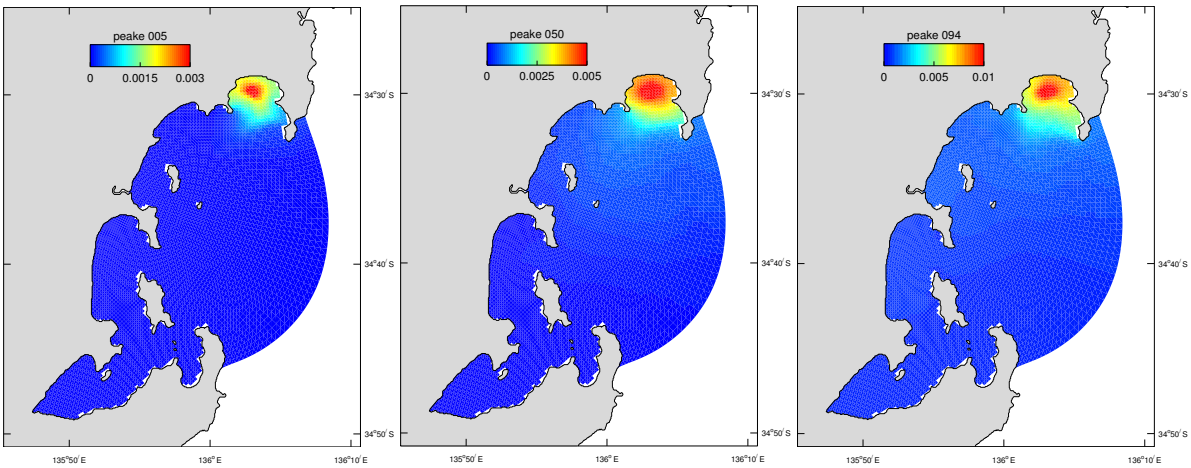

(a) 5 percentile (b) Median (c) 95 percentile

Figure 8.5.4. Quasi-steady state tracer distribution for Peake Bay release.

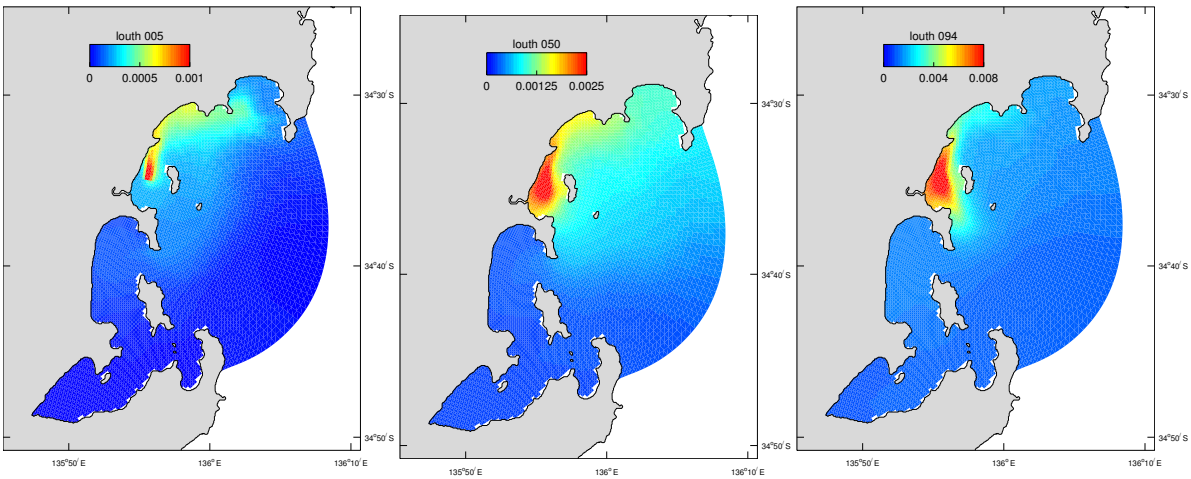

(a) 5 percentile (b) Median (c) 95 percentile

Figure 8.5.5. Quasi-steady state tracer distribution for Louth Bay release.

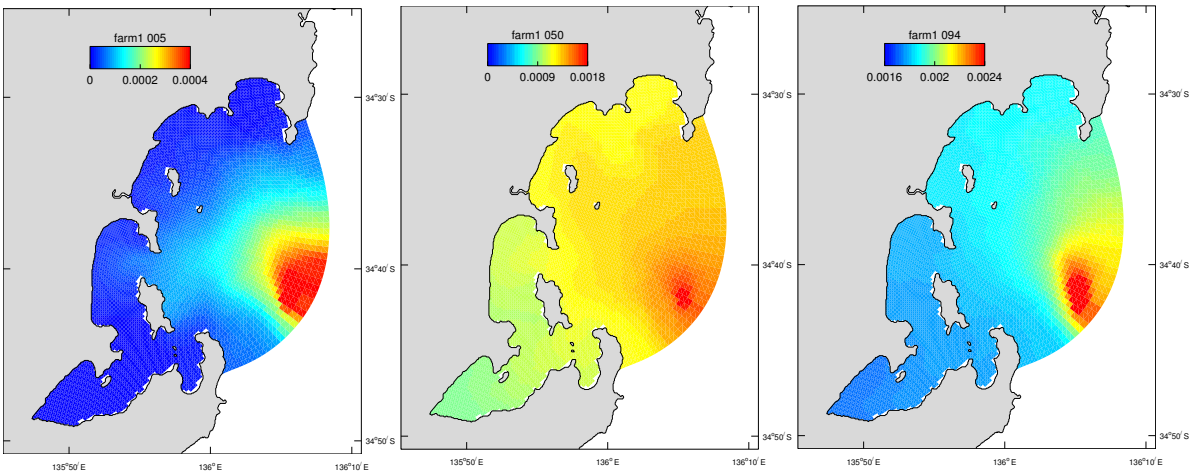

(a) 5 percentile (b) Median (c) 95 percentile

Figure 8.5.6. Quasi-steady state tracer distribution for Farm #1 release.

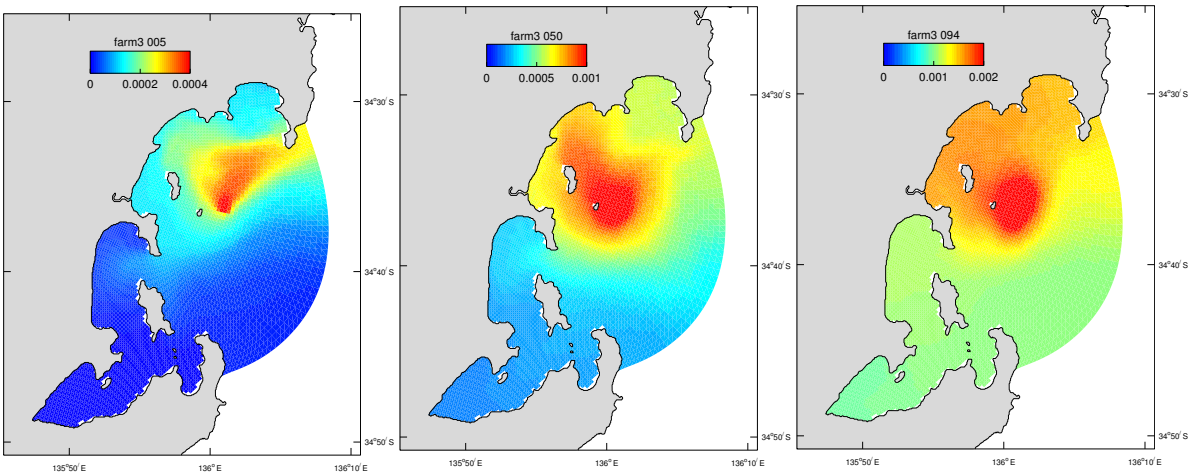

(a) 5 percentile (b) Median (c) 95 percentile

Figure 8.5.7. Quasi-steady state tracer distribution for Farm #3 release.

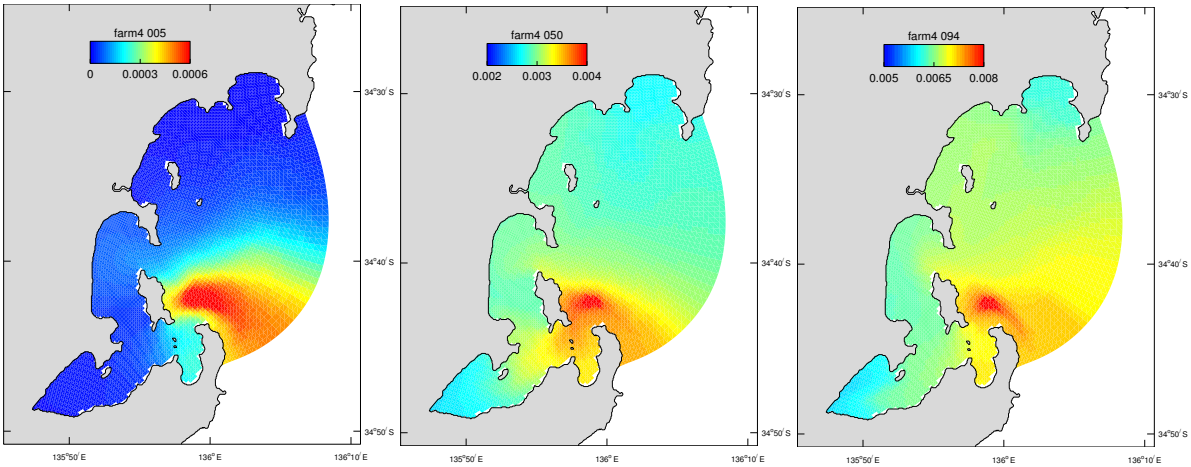

(a) 5 percentile (b) Median (c) 95 percentile

Figure 8.5.8. Quasi-steady state tracer distribution for Farm #4 release.

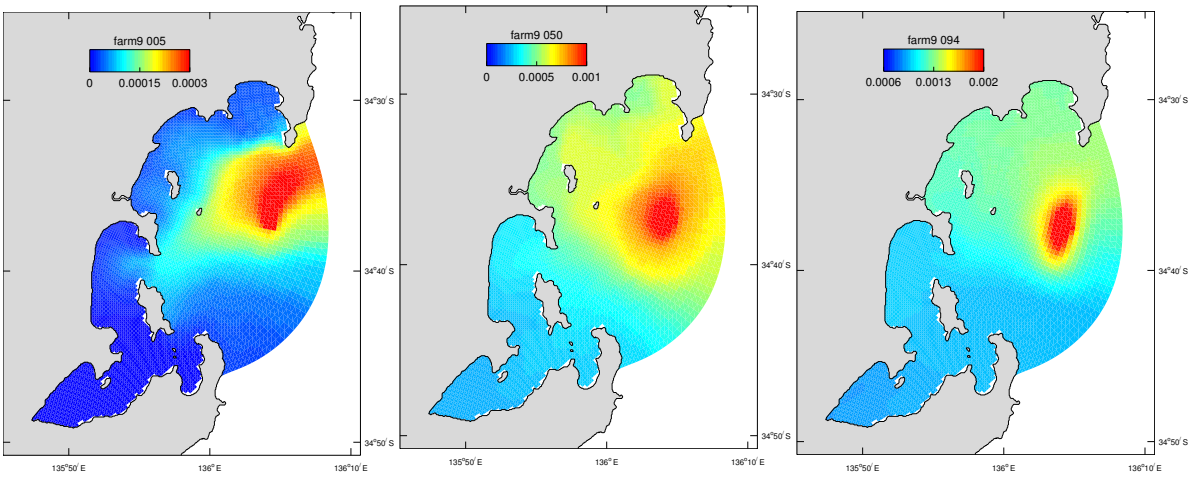

(a) 5 percentile (b) Median (c) 95 percentile

Figure 8.5.9. Quasi-steady state tracer distribution for Farm #9 release.

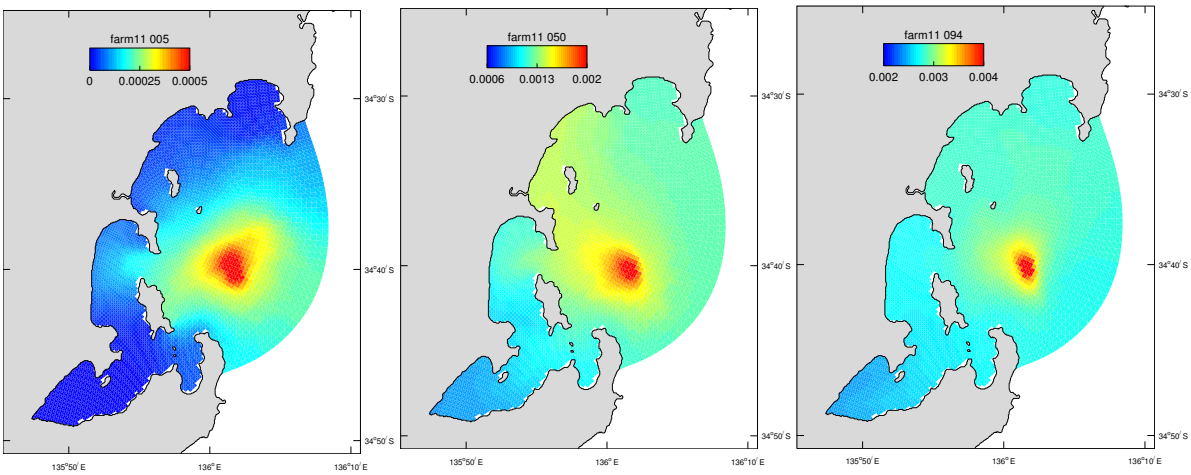

(a) 5 percentile (b) Median (c) 95 percentile

Figure 8.5.10. Quasi-steady state tracer distribution for Farm #11 release.

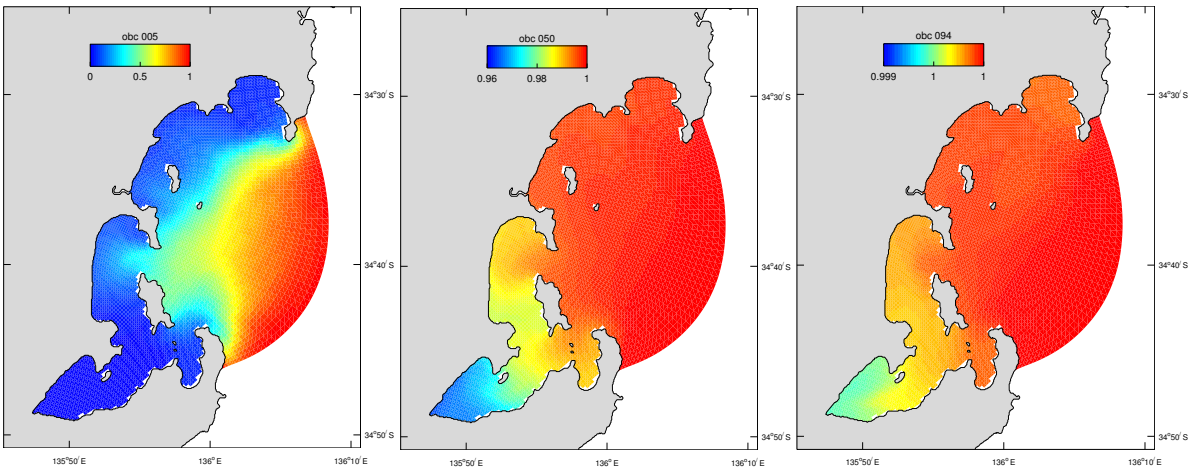

(a) 5 percentile (b) Median (c) 95 percentile

Figure 8.5.11. Quasi-steady state tracer distribution for Open boundary release.

The distributions above indicate that tracer released in the Proper Bay / Port Lincoln area tends to remain in that area; similarly tracer released in Louth or Peake Bays remains restricted to those areas. Tracer released offshore of Boston Island is distributed throughout most of the domain, although concentrations are lower indicating a larger amount of tracer is removed from the system. Connectivity therefore appears to be divided into three separate regions:

1. Landward of Boston Island and Proper Bay, with poor connectivity with the rest of the domain,
2. Louth and Peake Bays, with poor connectivity with the rest of the domain,
3. Regions outside these bays and offshore of Boston Island, with good connectivity with the remainder of the domain, but subject to greater flushing.

The farm sites having tracer released offshore of Boston Island which impinge on the bay regions tend to assume the character of those respective regions; e.g. farm #3 release near

Louth / Peake Bays is less well connected with Proper Bay than tracer released closer to that region (farm #4). Tracer input along the open boundary rapidly finds its way throughout the whole domain, with Proper Bay being the least accessible region. The connectivity of the domain as diagnosed from the point source releases is consistent with the mean depth averaged flow schematic of Figure 8.2.11, where circulation cells are established in Boston / Proper and Louth / Peake Bays, fed by south to north throughflow in the deeper parts of the domain seaward of Boston Island. The circulation cells are of a closed nature and do not promote good connectivity with the remainder of the region.

8.6. Connectivity

The connectivity of the domain can be examined by observing the behaviour of neutrally buoyant particles released from the same locations and depths as the point source releases in Section 8.5. The particles were released at a rate of 2 particles hour^{-1} from an initial pool of 10,000 particles. These particles were subsequently advected with the circulation to provide insight into how various regions of the domain are connected. The particles are also subjected to random motion representing the effect of diffusion (i.e. sub-grid scale effects). Therefore, any two particles released from the same place at the same time are expected to undergo different trajectories due to this random motion. When a particle crosses the offshore open boundary it is placed in the initial pool for subsequent re-release. The particle distributions after 12 months of simulation are displayed in Figures 8.6.1 to 8.6.9. This distribution is the projection of particles at all depths onto the surface. Particles are colour coded according to their age since being released over the range 0 – 30 days (i.e. blue particles are 0 days old, red particles are > 30 days old).

The connectivity of the domain inferred from the particle distributions is in agreement with the point source distributions (Section 8.5). Particles released at Port Lincoln in Boston Bay are confined to that area, whereas those released in Louth Bay remain in the northern vicinity of the domain. Those released near the open boundary (Farm #1 and #9) are rapidly removed, with few particles distributed throughout the domain. Particles within the domain for these release sites are associated with an older age. These distributions are consistent with the depth averaged net flow conceptualized in Figure 8.2.11. The average age of the 122,428 particles that exited the domain was 19.9 days, which is indicative of the flushing time for the whole domain.

Note that these images represent a snapshot of the particle distributions, and will vary in accordance with the forcing in effect. An animation of the particle motion over time best conveys the connectivity of the region, although observation of isolated particle trajectories does supply insight into the dynamics of the system. Trajectories were plotted during spring and neap tides for one tidal cycle (low water to low water). Note that circles correspond to the start of the trajectory and squares to the end in these figures, with the net displacement of start and end locations being indicative of the residual flow. Particle trajectories are superimposed on the surface from all depth levels.

Trajectories under the influence of spring tides show the oscillatory nature of the tide (Figure 8.6.10), especially near the offshore boundary. Gross displacements may be large, over 8 km, but small net displacements are observed. Neap tide trajectories exhibit little tidal motion, with particle displacement dominated by the wind (Figure 8.6.11 on 7 January 2006 for an easterly wind, showing net westward motion). Dodge tides reveal a similar situation to neap tides (Figure 8.6.12).

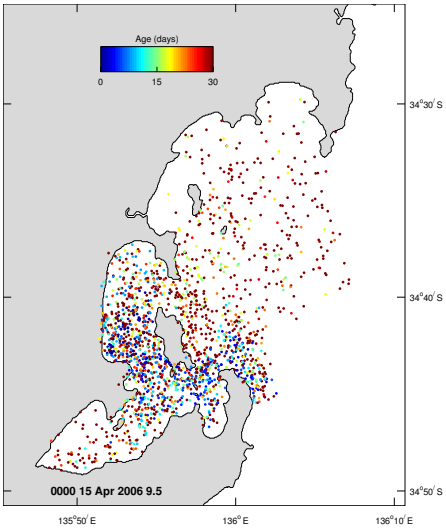

Figure 8.6.1. Particle distribution by age for particles released at Port Lincoln.

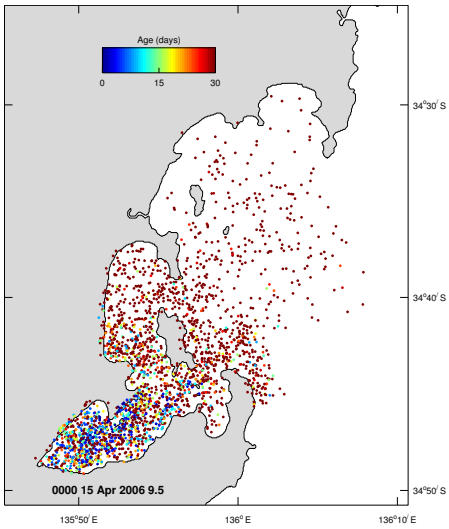

Figure 8.6.2. Particle distribution by age for particles released at Proper Bay.

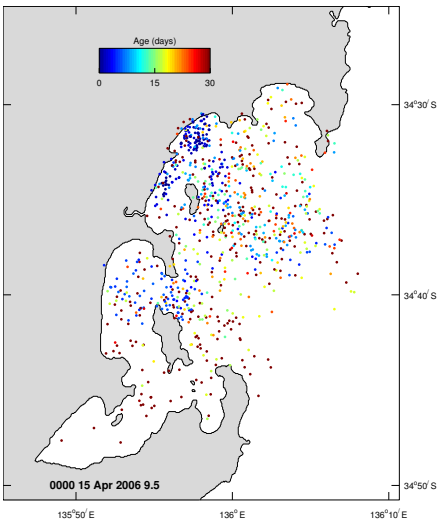

Figure 8.6.3. Particle distribution by age for particles released at Louth Bay.

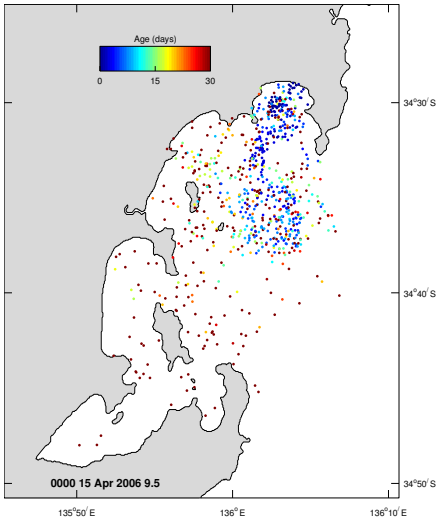

Figure 8.6.4. Particle distribution by age for particles released at Peake Bay.

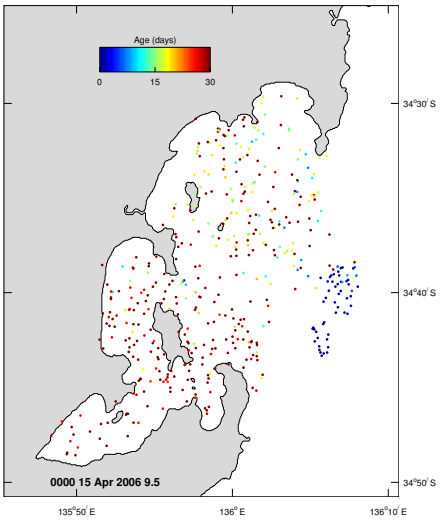

Figure 8.6.5. Particle distribution by age for particles released at Farm #1.

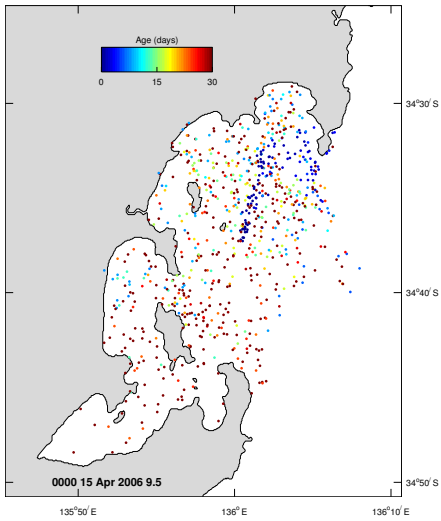

Figure 8.6.6. Particle distribution by age for particles released at Farm #3.

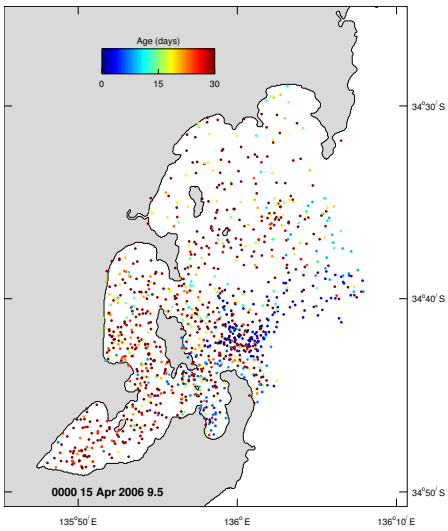

Figure 8.6.7. Particle distribution by age for particles released at Farm #4.

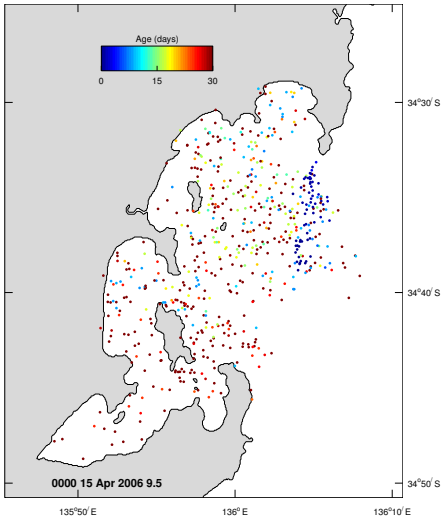

Figure 8.6.8. Particle distribution by age for particles released at Farm #9.

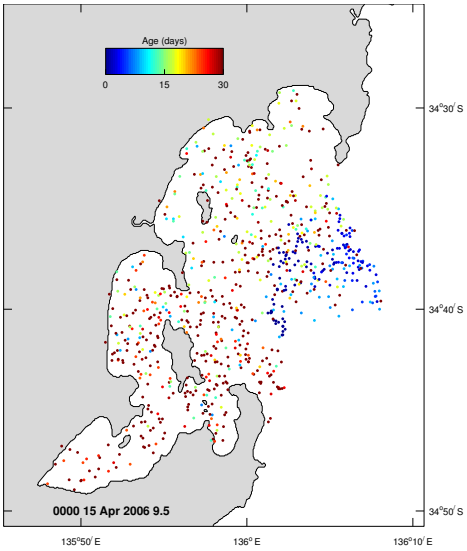

Figure 8.6.9. Particle distribution by age for particles released at Farm #11.

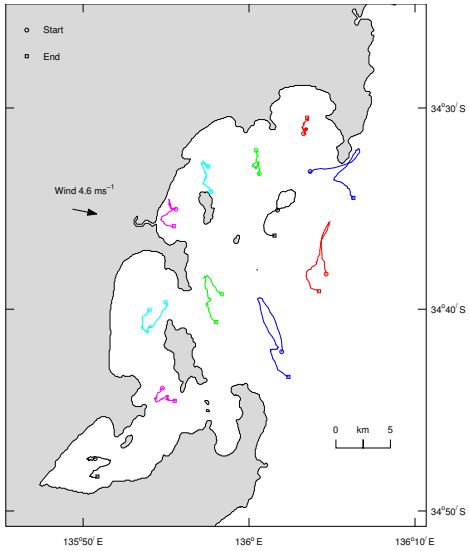

Figure 8.6.10. Spring tide trajectory, 22 Oct.

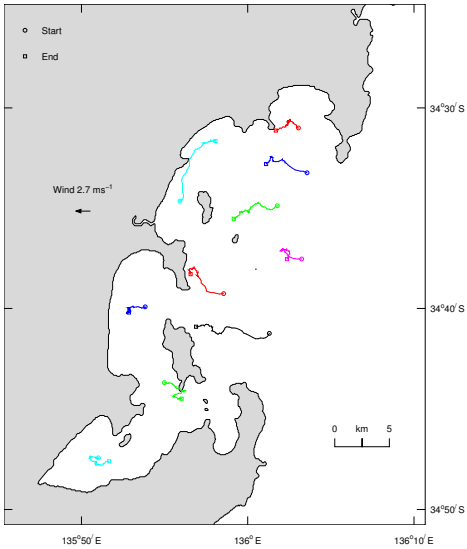

Figure 8.6.11. Neap tide trajectory, 7 Jan.

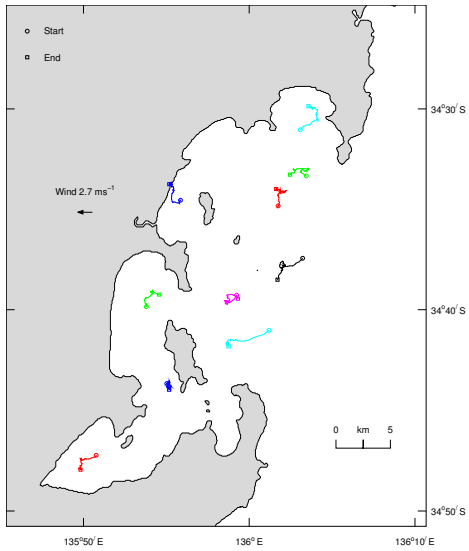

Figure 8.6.12. Dodge tide trajectory, 8 Jan.